207L CELLULAR NEUROSCIENCE LABORATORY CLASS

21st Annual Edition - March 7 – 16, 2005

Assigned Experiments

Compound action potential of sciatic nerve

Intracellular recording from muscle end-plate : mepps/epps

Voltage clamp of *Xenopus* oocytes

Extracellular field recording from rat hippocampal slices

Elective experiments (choose 1 or 2 experiments, as time and equipment permit)

IP_3/Ca^{2+} second messenger system – Ca^{2+} imaging / flash photolysis of caged IP_3

Patch clamp recording

Demonstrations

Whole-cell patch and Ca^{2+} imaging of neurons in brain slice

Single-channel imaging

Student presentations (Wednesday afternoon, March 16)

Appendices

A. Time distribution of mepps.
B. Statistical analysis of quantal transmitter release.
C. Equipment for intracellular recording.
D. Dissection of frog sartorius nerve/muscle preparation.
E. mRNA from brain induces membrane channels in oocytes.
F. Schematic of voltage clamp.
G. Use of caged compounds and fluorescent Ca^{2+} indicators.

EXPERIMENTS

1) Sciatic Nerve

Mount the nerve so that the stimulating cathode and the earthed recording lead are innermost. It is best to record from the thinner end of the nerve while stimulating the thicker end. Use AC-coupled recording; if the recorded potential still drifts about, clean the electrodes with fine emery cloth. Do not allow the nerve to dry out.

For diphasic recording, keep the recording electrodes 2 mm apart. Trigger the oscilloscope from the stimulator, with a suitable delay between triggering pulse and stimulus. Increase the stimulus strength (at a fixed duration of 0.1 - 0.2 msec) and determine the relation between intensity of stimulus and amplitude of the compound action potential. Determine the conduction velocity by varying the distance between the recording lead and the stimulating cathode. Alter the electrode separation, and measure the time between the stimulus and the maximum rate of rise of the spike for each distance.

Repeat with monophasic recording. For monophasic recording keep the outer recording electrode on a freshly crushed part of the nerve near its distal end.

Refractory period - With monophasic recording use supramaximal stimuli (stimulus strength about twice that needed for a maximal response). Vary the interval between the two stimuli. Super-impose several intervals on one photograph.

2) Resting potential of muscle fiber

Dissect out the sartorius muscle, as described in appendix D (note that for this and experiment 3 there is no need to dissect out the nerve together with the muscle).

Determine the value of resting potentials in 10-20 fibres; calculate mean and S.E. of mean. The normal value is about -80 mV. Lower values suggest a poor preparation or bad impalements.

Penetration of fibres is best done by first lowering the tip of the microelectrode until it is just above a selected fibre. The gain of the recording system should be at 20 mV/cm, and any offset potential should be backed off to zero. Then slowly lower the electrode, watching the oscilloscope, not the muscle. The potential should abruptly change to a new level; a slow change indicates a poor penetration. See appendix C for more information on microelectrodes.

3) Miniature end-plate potentials (m.e.p.p.s)

Mount the muscle with its deep surface upwards, and bathe in a Ringer solution containing 10^{-6} g/ml prostigmine (this inhibits hydrolysis of ACh, and thus increases the size of m.e.p.p.s). Penetrate fibres in the region where you expect to find end-plates (about 1/3 of the muscle length from the pelvic end), and record at a gain of 0.5 or 1mV/cm. If the electrode is near an endplate, transient random potentials may be observed - these are the m.e.p.p.s. Note their shape and rate of occurrence. If the rising phases are slow and rounded, the electrode is some distance from the endplate. If they are too infrequent (say less than one every 2 sec), then it may be convenient to increase the frequency by adding

sucrose up to a final concentration of about 30 mM.

When you obtain good m.e.p.p.s, take pictures of their time course by photographically superimposing several sweeps. Plot histograms showing the distribution of intervals between m.e.p.p.s, and statistically analyze this to see if the m.e.p.p.s occur at random intervals (See appendix A).

4) End-plate potentials (e.p.p.s.)

Mount the muscle as before and position the nerve across the stimulating electrodes. Apply a stimulus of about 0.1 ms and less than one volt to make sure that muscle twitch is present.

Place the preparation in a Ca-free medium + 2mM Mg^{2+} for about 1 hr. Change the medium at least twice during this time to remove the Ca^{2+}. Then add prostigmine (10^{-6} gm/ml) and some Ca^{2+} to the bathing medium (0.15 mM Ca gives mean quantal content, $m \approx 0.2$; 0.25 mM gives $m \approx 1.0$; 0.4 mM Ca gives $m \approx 5$). Apply a stimulus to check that muscle twitch is absent.

Penetrate a muscle fibre in the endplate region (m.e.p.p.s should be detectable) and stimulate the nerve to produce an e.p.p. Reduce the voltage of the stimulus to determine the threshold for the e.p.p. Set the voltage to give a supramaximal stimulus of three times this size so that any failure to generate an e.p.p. does not result from failure of the nerve action potential. For the optimal calculation of a Poisson distribution, about 10 - 30% of nerve impulses should fail to release transmitter. Stimulate the nerve once every 3 secs (or every 2 secs) to obtain 150 - 200 e.p.p.s. Stimulation at a higher rate than this will cause facilitation of transmitter release. Ideally m.e.p.p.s (~100) should be recorded

both before and after taking e.p.p.s in case the resting potential of the cell changes during the experiments. Some details of use for calculating a Poisson distribution are given in Appendix B.

Take a series of records with double nerve stimuli delivered at a fixed interval (about 3-10 msec) and giving noticeable facilitation. Keep the rate of paired stimuli constant at about 1 pr/3 sec. Compare the amplitude distribution of responses to the first and second stimulus of the pair.

5) **Voltage clamping of endplate currents**

With the muscle in prostigmine Ringer, insert a recording microelectrode close to an endplate (m.e.p.p.s should have a rapid rising phase). Then insert a second electrode into the same fibre within a few hundred microns. Record from this electrode to monitor the penetration, and then switch it for use as the current passing electrode of a voltage clamp. Appendix F shows a schematic of the clamp circuit. Before turning on the clamp, set the command voltage on the calibrator to equal the resting potential. Never depolarize the fibre below about -60 mV, or it will contract, and ruin all your hard work! Adjust the clamp gain so that changes in command potential produce almost no shift in the voltage trace on the oscilloscope (in clamp mode this monitors the error between the desired and actual membrane potential). The current monitor trace should shift as the command potential is changes, and from this you can calculate the input resistance of the fibre.

Rapid blips of current should be visible on the monitor, of 2-3 nA size; these are the m.e.p.c.s (miniature endplate currents). Note that the voltage clamp is more susceptible to noise and 60 Hz interference than potential recordings. You may have to improve shielding etc. to get the baseline noise low enough to see the m.e.p.c.s clearly. Investigate the effects of changes in membrane potential on the amplitude and decay time course of the m.e.p.c.s You should be able to determine the reversal potential of the ACh channel (by extrapolation), the conductance change induced by a quantum of ACh, and the mean channel lifetime at various potentials.

6) **$InsP_3/Ca^{2+}$ second messenger pathways in oocyter**

Many neurotransmitter receptors exert their actions via a signalling pathway involving intracellular messengers. One way of studying there pathways is to bypass the receptors and directly introduce the messengers into a cell. The procedure is particularly easy in the large oocytes of Xenopus; which possess a phosphonositide pathway in which inositol trisphosphate (IP_3) causes liberation of intracellular calcium, leading finally to the opening of calcium-dependent chloride membrane channels. Thus, injection of calcium directly evokes a chloride current, while injection of IP_3 gives a current as a result of the release of calcium from intracellular stores.

A more elegant way to control level of $InsP_3$ in a cell is by the use of 'caged' $InsP_3$. This is a chemical derivative of $InsP_3$ that is physiologically inactive, and can be loaded into a cell without producing an effect. However, the compound is photolabile, so that flashes of ultra-violet light can then be used to liberate free $InsP_3$ within the cytosol. Furthermore, instead of monitoring Ca^2 release by recording Ca^2-activated Cl^- current, a more direct approach is to use fluorescent Ca^2-sensitive dyes loaded into the cytosol. Details of both these technique are given in Appendix G.

Injection of caged $InsP_3$ and Ca^{2+} indicator dyes from a standard glass micro-pipette is done by applying pneumatic pressure pulses, using an electrically activated valve to control the pulse direction, and a regulator to set the compressed air pressure. The amount of fluid ejected can be estimated by measuring (with a calibrated graticule

in the dissecting miscoscope) the diameter of the fluid droplet expelled with the pipette tip in air. Regular pipettes are too sharp to eject much fluid; after pulling and filling a pipette the tip will need to be broken (gently) so as to be big enough to pass fluid, but still sharp enough to penetrate the cell. Recording from the oocyte can be done using either a single voltage-recording electrode, or a two-electrode voltage clamp. Insertion of the injection pipette is monitored as a sharp fall in resting potential, or (in voltage-clamp) a sharp increase in holding current. Injection pipettes should be filled with 5mM $CaCl_2$ or 100μM IP_3 (together with 50 μM EDTA to chelate any contaminating calcium).

7) Brain neurotransmitter receptors transplanted to the Xenopus oocyte

Most of our knowledge about synaptic transmission derives from experiments on the neuromuscular junction. One reason for this is that muscle cells are large, and thus easy to penetrate with micro-electrodes. In contrast, the small neuronal cells in the central nervous system are much less amenable to electrophysiological techniques, and less is known about the wide variety of neurotransmitter receptors which they possess.

A new technique has recently become available which largely overcomes these difficulties. This involves the injection of messenger RNA derived from brain into oocyte cells of Xenopus laevis. Messenger RNAs coding for many transmitter and voltage activated membrane channels are faithfully translated and processed by the oocyte, so that it will show responses similar to those in the 'native' neuronal cells of the brain. The study of these exogenous

transmitter receptors is, however, much simplified when they are expressed in the large (ca 1 mm) spherical oocyte cells. (See Appendix E for more details.)

You will be supplied with oocytes injected with mRNA from rat brain. These should have developed receptors to many transmitters (including serotonin, GABA, kainate and glutamate), which can be applied by a bath perfusion system. Note that the chloride equilibrium potential in the oocyte is about -20 mV, as compared to about -90 mV in neurones. Thus, transmitters (such as GABA) which open chloride channels and tend to have hyperpolarizing (inhibitory) actions on neurones, will tend to depolarize the oocyte.

8) Patch-clamp of single channels in the membrane of Xenopus oocytes.

Patch clamp recording has revolutionized our understanding of the ways in which membrane channels operate, by allowing us to directly record currents through single channel molecules. In this experiment you will be able to record from a variety of different channels in the oocyte, both those which are normally present and (if you are very lucky) exogenous channels expressed by injected mRNA. The oocyte is a fairly easy cell to patch clamp, as once a clean membrane surface is prepared it is remarkably simple to form tight seals onto the patch pipette. The most prominent type of channel you are likely to see is a Na^+/K^+ channel activated by stretch (suction on patch pipette). Details for making patch pipettes and preparing oocytes will be given during the course.

APPENDIX A

Time distribution of m.e.p.p.s

If the m.e.p.p.s occur at random times, then the number observed in any given time interval (eg 1 sec) should follow a Poisson distribution;

$$Px = \frac{m^x}{x!} e^{-m}$$

where P_x = probability of observing any any particular number x

m = mean number of m.e.p.p.s per interval

By measuring the number of m.e.p.p.s which occur in each of 50-100 consecutive time intervals (0.5 - 5 sec depending on m.e.p.p frequency), you can check how well your data fit the theoretical Poisson distribution, using an χ^2 test.

An alternative method of analysis is to measure the time intervals between several hundred consecutive m.e.p.p.s, and plot a histogram of the frequencies of the various intervals. If m.e.p.p.s occur randomly, these should follow an exponential distribution:

$$n = N\Delta t/Te^{-t/T}$$

where n = number of observed intervals of width Δt

N = total number of intervals

T = mean interval

APPENDIX B

Statistical analysis of transmitter release

Three methods of obtaining mean quantal content, m.

1.	Direct method	m =	(mean e.p.p./mean m.e.p.p)
*2.	Failures method	m =	ln (no. impulses / no. failures)
*3.	Coefficient of variation	m =	(mean e.p.p./S.D. e.p.p.)^2

*Theses two methods assume that Poissons's law applies to transmitter release.

Testing fit of Poisson's theorm

If we assume that Poisson's law applies and have calculated m by one of the above methods it is possible to predict the no. of responses to nerve impulses which will contain 0,1,2,3 ...k, quantal components.

i.e. n_0, n_1, n_2, n_3 ..., n_k.

Where

$n_0 = Ne^{-m} \quad \ldots e^{-m}$ (from tables) gives the proportion of N (total impulses) made up by n_0

$n_1 = mn$

$n_2 = (m/2)n_1$

$n_3 = (m/3)n_2$

$n_k = (m/k)n_{k-1}$

Obtaining quantum size, q, when m.e.p.p.s not available

Assuming Poisson's law applies it is possible to calculate the size of the quantum, q (i.e. the expected size of the m.e.p.p.) when m.e.p.p.s are not available.

1. $q = \frac{(\text{S.D.e.p.p.})^2}{\text{mean e.p.p.}}$

2. $q = \frac{\text{mean e.p.p.}}{m}$ ..... where m is obtained without m.e.p.p.s.

As these methods assume Poisson's law they cannot be used if testing for the validity of Poisson release.

Fitting Gaussian Curves to e.p.p. data

Assuming you have already managed to fit a Poisson, as above (and see Katz, N,M & S - p.134), then proceed as follows.

(1) Take a clean sheet of paper and draw up the magic table shown below at the top of it.

x/σ	0	0.2	0.4	0.6	1.0	2.0	3.0
$y\ \sigma$	.399	.391	.368	.33	.24	.05	.004

This table gives a series of points on the s.t.d. normal curve. All that is needed is to adapt this curve so that its area = no. of observations in one Poisson group (i.e. no. of responses involving a certain number, N of quanta), and its variance = variance of min e.p.p.s x N.

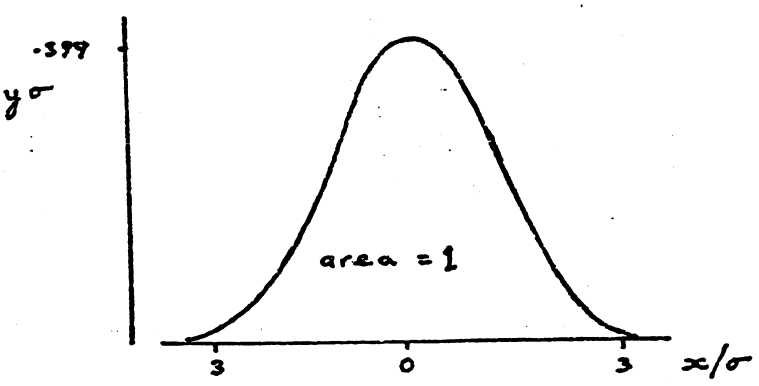

(2) Calculate variance of min e.p.p.'s, $\sigma^2 = \frac{1}{n} \sum_{i=1}^{n} (x_i - \bar{x})^2$

n = no. of observations, $\bar{x}$ = mean amplitude

(3) For the first Poisson group (i.e. responses involving one quantum) correct the figures in the x/σ column by multiplying by σ ($=\sqrt{\sigma^2}$).
Correct the figures in the $y\sigma$ column by multiplying by

$$\frac{n}{\sigma \times z}$$

where n = no. of observations in Poisson group
z = 1/width of chosen histogram block

(4) Repeat step (3) for the remaining Poisson groups, remembering that $\sigma = \sqrt{\sigma^2 \times N}$

(5) Plot the points obtained on top of the histogram of the experimental data. Only one side of the curves has been calculated, the other is a mirror image. The curves center about the points on the x axis which are multiples of the mean min e.p.p. amplitude.

(6) Join the points up to give a series of Gaussian curves, and find the theoretical amplitude distribution by adding these together.
See del Castillo & Katz, J. Physiol. 124, 560-573 for a full account.

APPENDIX C

Equipment for intracellular recording

The micro-electrodes for intracellular recording consist of fine glass capillaries pulled to a tip diameter of $\sim$0.5 µm and filled with a 3M solution of KCl. The glass tubes contain a glass fibre fused to the inside, which facilitates filling, and the KCl solution is simply injected into the back of the micro-electrode using a fine hypodermic needle. Electrodes should have a resistance of between about 5 to 30MΩ, and this high resistance requires the use of a special F.E.T. input amplifier with an input impedence of $>10^{12}\Omega$.

The high resistance of micro-electrodes creates two main problems.

(i) Johnson noise is generated by thermal motion of ions in the tip. This can be seen by recording at a high gain with the electrode in the bath, and should be a few hundred µV in amplitude. The noise is proportional to electrode resistance, and a sudden disappearance of the noise is a good indication of a broken electrode tip!

(ii) Any stray capacitance to earth from the micro-electrode or F.E.T. amplifier will form an RC circuit with the electrode resistance, and will attenuate high frequency signals. To see this effect, apply a voltage pulse from the stimulator to the electrode, and look at the rising phase of the pulse. Compare the pulse recorded from the electrode, with that recorded directly from the stimulator output. Much of the capacitance arises between the electrode and the bathing solution, and will be increased if the electrode is lowered deeper into the solution. You should be able to calculate the capacitance in the circuit, from the degree of rounding of the square plus.

(iii) Unless carefully screened in a Faraday cage, the recording system will pick up vast amounts of mains interference (60 Hz and 120 Hz). When earthing equipment, make sure that each item is connected to earth via only <u>one</u> route (to avoid 'hum loops').

APPENDIX D

Dissection of frog sartorius with nerve

1. Stun, decapitate and pith.
2. Eviscerate. Take care not to damage lumbar spinal nerves (under the kidneys).
3. Cut off upper half (above origin of the sciatic plexus).
4. Skin lower part.
   Pin to frog board, frog on its back
5. Tie thread around lumbar spinal nerves close to spinal cord on one side.

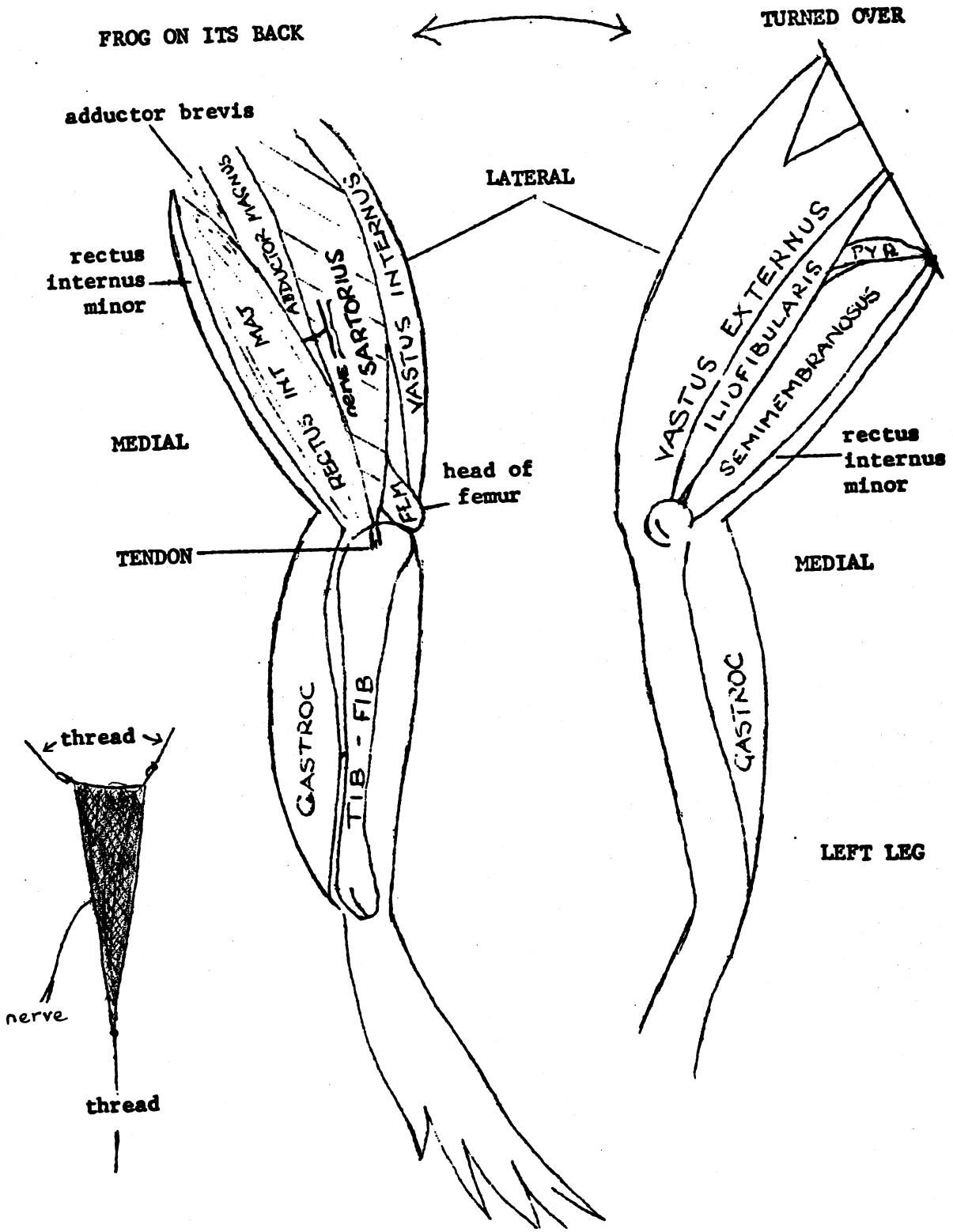

6. Find sartorius tendon at knee. Cut off connective tissue so that fine forceps can be passed under tendon and tie thread around it without touching muscle fibres at any stage. Detach tendon.

   KEEP PREPARATION MOIST BY IRRIGATING WITH RINGER THROUGHOUT DISSECTION.

7. Note nerve entry to sartorius. Detach the muscle medial to the sartorius, the rectus internus major, from the knee upwards. It runs by the side of the sartorius at first, then by the side of the adductor magnus. In removing the rectus take special care at the sartorius nerve entry; the nerve lies just below the superficial connective tissue. The rectus nerve must of course be cut to remove the muscle. You should now be able to see the sartorius nerve lying on the surface of the adductor magnus, more of which has been exposed, and also the semitendinosus muscle with a prominent tendon to the knee (and two heads which will be seen at the next step).

   Remove the rectus internus minor if it has not come away with the major.

8. Cut the semitendinosus knee tendon and pull the muscle away from the frog. The sartorius nerve should now be seen making a sharp bend back towards the frog. Cut the nerve to the semitendinosus and remove the muscle, which can now be seen to fork. The sartorius nerve lies on the outer surface of the adductor magnus and the inner surface of the semimembranosus.

9. Remove the semimembranosus; this involves cutting under the sartorius nerve. When the semimembranosus is removed, the main trunk of the sciatic nerve can be seen, together with a fair length of the sartorius branch.

10. Free the sartorius muscle to the point of nerve entry. This will allow you to see if the muscle contracts when you test your dissection of the nerve, with Galvani forceps, at a later stage.

11. Detach nerves from spinal cord.

12. Turn frog over and remove urostyle. If you cut close to it on both sides, you will not damage the sciatic nerves. Bring thread through the hole made by the missing urostyle.

13. Turn frog over. Remove the stump of the semimembranosus and also the pyriformis muscle to expose the junction of the branch to the sartorius with the main sciatic nerve.

    The whole course of the sartorius nerve should be visible. Test the nerve with Galvani forceps applied to the sciatic. Cut branch going to the gastrocnemius. Dissect the nerve towards the sartorius muscle. The last few mm are usually rather firmly attached to the connective tissue of the adductor magnus, and should be left until the next stage.

14. Place frog on its back. Arrange the isolated portion of nerve so that it lies alongside the sartorius and at no time should tension be applied to the nerve. Cut carefully through connective tissue on either side of and below the muscle. Near its entry into the muscle the nerve may be dissected together with a small piece of the underlying muscle.

15. Continue the dissection of the sartorius muscle, freeing its edges up to the pelvic insertion. Tie threads around the connective tissue at each side of the pelvic insertion. Take care that no sartorius muscle fibres are ligated. With scissors cut the insertion along the bone cutting, if necessary, into the cartilage to avoid damaging the muscle. Excess tissue can be trimmed away from the isolated preparation. When the preparation is to be mounted for recording, have the muscle support the thin, fragile portion of the nerve.

Appendix E

Messenger RNA from human brain induces drug- and voltage-operated channels in *Xenopus* oocytes

C. B. Gundersen, R. Miledi & I. Parker

Department of Biophysics, University College London, Gower Street, London WC1E 6BT, UK

Sodium channels and receptors to serotonin and kainate were 'transplanted' from human brain into frog oocytes, by isolating messenger RNA from a fetal brain, and injecting it into Xenopus laevis *oocytes. The mRNA was translated by the oocyte and induced the appearance of functional receptors and channels in its membrane. This approach renders drug- and voltage-operated channels of the human brain more amenable to detailed study.*

FOR obvious reasons, it is important to know how neurotransmitter receptors and channels function in human brain neurones; but these cells are not easily amenable to the necessary experimental approaches. One possibility would be to culture human brain cells[1,2] and study them with electrophysiological and biochemical techniques[3–6]. Alternatively, one might purify the receptor and channel proteins from human neuronal membranes, and study their function after incorporation into artificial membranes, as has been done with other systems[7,8]. We decided on a different approach, one that may allow us to study not only the functioning of receptors and channels, but also the way in which their constituent proteins are synthesized, processed and incorporated into the cell membrane. Essentially, the method consists of isolating messenger RNA (mRNA) from the human brain, and injecting it into oocytes of *Xenopus laevis*. This induces the appearance of receptors and channels in the oocyte membrane, in the same way as was done previously with mRNA from chick[9] or rat[10–12] brains.

Membrane channels induced by mRNA

Injection of mRNA derived from fetal human cerebral cortex into *Xenopus* oocytes caused the synthesis, and incorporation into the membrane, of channels which could be activated either by drugs or by voltage changes. These included voltage operated sodium channels (Figs 1, 2), and receptor–channel complexes activated by serotonin (Fig. 3) and kainate (Fig. 4). All of them resulted from the injection of exogenous mRNA, since most injected oocytes gave responses, whilst control (non-injected) oocytes from the same donors did not show responses (Table 1).

Two further lines of evidence indicate that the proteins forming these membrane channels arose directly from the translation of the human mRNA by the oocyte, and not because the injection of foreign mRNA caused the oocyte to transcribe the appropriate messengers from its own genome. First, oocytes developed the voltage- and drug-activated responses even after they had been exposed continuously to actinomycin D (50 μg ml^{-1}) to inhibit synthesis of mRNA[13]. Second, the responses still developed in oocytes which had been enucleated[12,14] before injection of human mRNA.

Voltage-activated sodium current

A few days after injecting the oocytes with human cerebral cortex mRNA, depolarizing pulses elicited an inward membrane current (Fig. 1*a*). In contrast, non-injected oocytes from these donors showed predominantly passive (ohmic) currents. Figure 1 illustrates the current–voltage relationship for the inward current. The current first became detectable when the membrane potential was stepped from −100 to about −40 mV, and increased with increasing depolarization to reach a maximum at about −10 mV. With further depolarization the current declined, and was reduced to about zero at a potential of +60 mV.

The peak amplitude of the inward current elicited by depolarization was reduced if external sodium was partially substituted with Tris or tetraethylammonium ions. Furthermore, tetrodotoxin (TTX) readily abolished the inward current (complete block with 300 nM, half block with 10 nM). All this indicates that sodium is the main ion responsible for the inward current. Manganese (5 mM) also reduced the inward current, but this effect probably arises from a change in the characteristics of the sodium channels, rather than from a blockage of calcium channels[11,15].

The decay of the sodium current in oocytes injected with human cerebral cortex mRNA often showed two time courses. For example, in the upper record in Fig. 2*a*, the current shows an initial rapid decline, followed by a slower decay. During repetitive activation, the slow component of the decay 'fatigued' more readily than the fast component. This is evident in Fig. 2*a*. where two depolarizing pulses of 900 ms duration to a potential of −10 mV were separated by an interval of 100 ms. The slow component was strongly reduced during the second pulse, whilst the fast component appeared little changed.

Sodium currents induced by rat brain mRNA show a similar, two-component decay[11], but with a time course approximately three times faster. Mean values for the half decay time of sodium currents measured in oocytes from the same donor (at −10 mV and 12–15 °C) were: human cortex, 13.7 ± 1.3 ms (s.e.m., 18 oocytes; rat brain, 4.8 ± 1 ms (6 oocytes).

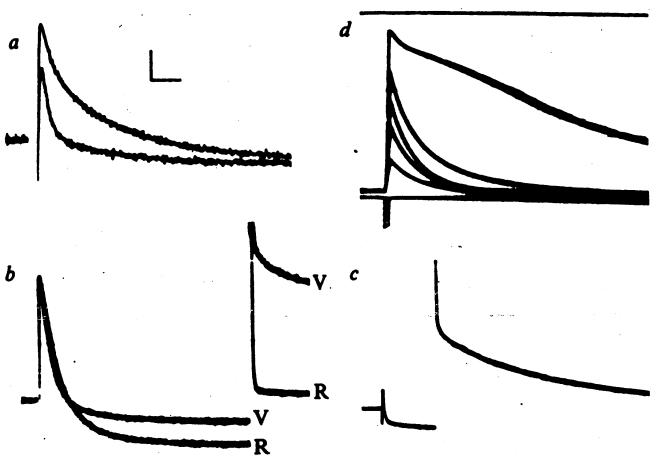

Fig. 2 Effects of repeated stimulation and of veratrine on the decay of the sodium current in oocytes injected with human cerebral cortex mRNA. *a*, Superimposed records showing membrane currents elicited by a pair of depolarizing pulses to −10 mV, from a holding potential of −100 mV. Pulse duration was 900 ms and the pulses were separated by an interval of 100 ms. The oocyte had been injected with human cortex mRNA and was treated with collagenase. Temperature, 15 °C. Calibration bars, 50 nA and 10 ms. *b*, *c*, Effects of veratrine on the sodium current elicited by a depolarizing pulse to 0 mV. Calibration bars are 50 nA and 50 ms in *b* and 100 nA and 200 ms in *c*. Traces marked R and V in *b* were obtained respectively before and after adding veratrine (0.5 mg ml^{-1}), whilst the trace in *c* shows the tail current in the presence of veratrine on a slower sweep speed. *d*, Action potential elicited in the presence of veratrine from the same oocyte as in *b*, *c*. Traces show (from top to bottom) 0 mV potential reference; membrane potential; and current injected into the oocyte. A steady current was passed to hold the membrane potential at about −100 mV, and responses are shown to a series of depolarizing current pulses of increasing intensity. The largest pulse triggered a graded regenerative response. Calibration bars, 20 mV (membrane potential), 500 nA (current monitor) and 500 ms. Temperature in *b*–*d* was 12 °C.

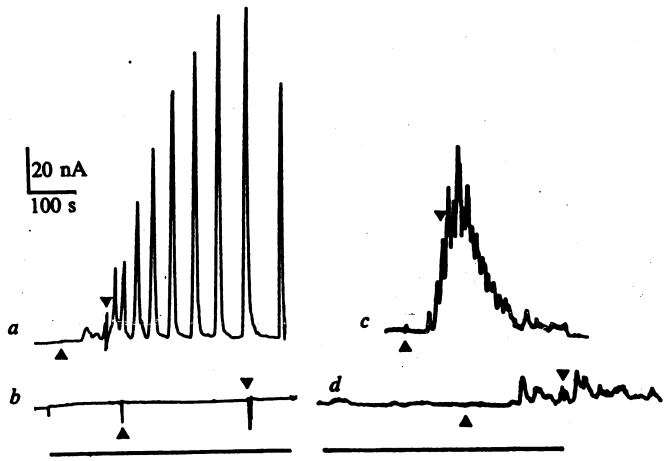

Fig. 3 Oscillatory membrane currents elicited by serotonin in oocytes injected with mRNA from human cerebral cortex. All records were obtained with the oocytes clamped at a potential of −60 mV so as to be away from the equilibrium potentials for sodium, potassium and chloride ions[21]. Serotonin was applied by bath perfusion, beginning and ending as indicated by the arrows. *a*, Response to serotonin recorded from an oocyte in normal Ringer's solution. *b*, Lack of response when serotonin was applied in the presence of methysergide. The bar indicates the duration of methysergide application. The concentration of serotonin was 10^{-6} M in both records, and the concentration of methysergide was 10^{-5} M. Temperature 14 °C. *c*, *d*, Reduction of size of the serotonin response by lysergic acid diethylamide. Serotonin was applied at a concentration of 5×10^{-7} M in both records, and lysergic acid diethylamide was added at a concentration of 2×10^{-6} M for the time indicated by the bar in *d*. Temperature, 11 °C.

nature of the currents (Fig. 3). In these respects, the responses are quite different from the smooth currents elicited by activation of γ-aminobutyric acid (GABA), kainate or nicotinic acetylcholine (ACh) receptors incorporated into oocytes following injections of the appropriate mRNA[9,13,20]. They do, however, resemble the oscillatory currents elicited by serotonin in oocytes injected with rat brain mRNA[10], as well as the currents elicited by activation of muscarinic ACh receptors[21] and glutamate receptors[12]. In the present experiments, application of ACh and glutamate to oocytes, which showed good sensitivity to serotonin following injection of human mRNA, did not elicit any appreciable currents. Thus, the serotonin responses probably involve a specific serotonin receptor.

The serotonin response was abolished by low concentrations ($<10^{-6}$M) of methysergide, a serotonin receptor antagonist[22] (Fig. 3*a*, *b*). The blocking action of methysergide appeared to be either irreversible, or only slowly reversible, since responses to serotonin were still blocked even after washing for an hour or more.

In contrast to the powerful blocking action of methysergide, the serotonin antagonists cyproheptadine and ketanserin[23] did not appreciably reduce the size of the response to 10^{-5} M serotonin when applied at a concentration of 10^{-6} M. Lysergic acid diethylamide (2×10^{-6} M) reduced, but did not completely abolish, the response to 5×10^{-7} M setotonin (Fig. 3*c*, *d*).

Membrane potential and serotonin current

The oscillatory currents induced by serotonin in oocytes injected with human cortex mRNA decreased in size as the membrane was depolarized and inverted direction at a potential of about −20 mV, which corresponds to the chloride equilibrium potential in *Xenopus* oocytes[21]. The equilibrium potential of the serotonin currents in oocytes injected with rat brain mRNA is also similar[10]. Thus, chloride is the main ion flowing through the channels activated by serotonin.

Depolarization beyond the equilibrium potential gave larger serotonin currents than corresponding steps in a hyperpolarizing direction, similar to the rectification seen with serotonin currents induced by rat brain mRNA[10]. This effect probably arose as a result of a voltage-dependent closing of the serotonin-activated channels, since a hyperpolarizing step applied near the peak of a serotonin-activated oscillation initially gave an increase in membrane current, which subsequently declined over a time course of a few hundred milliseconds.

Kainate receptor channels

Application of kainate to oocytes injected with human cerebral cortex mRNA elicited inward membrane currents (Fig. 4). These responses did not show oscillations, and were well maintained during kainate applications lasting several minutes. We did not observe clear responses to glutamate, even when applied at high concentrations (10^{-2} M) to oocytes which had a high sensitivity to kainate. This shows that in humans, as in rats[12], there is a kainate receptor which is distinct from glutamate receptors.

Currents elicited by different doses of bath-applied kainate are illustrated in Fig. 4. The minimal concentration required to give detectable responses was higher than for serotonin. For example, the oocyte illustrated in Fig. 4 gave a just detectable response at 10^{-5} M kainate, while a concentration of 5×10^{-4} M gave a maximal response. At low doses of kainate, a doubling in the concentration more than doubled the peak size of the response.

The reversal potential of the kainate-induced current (estimated by stepping the membrane to different potentials before and during steady kainate application) was about −10 mV. At voltages more negative than the equilibrium potential, the cur-

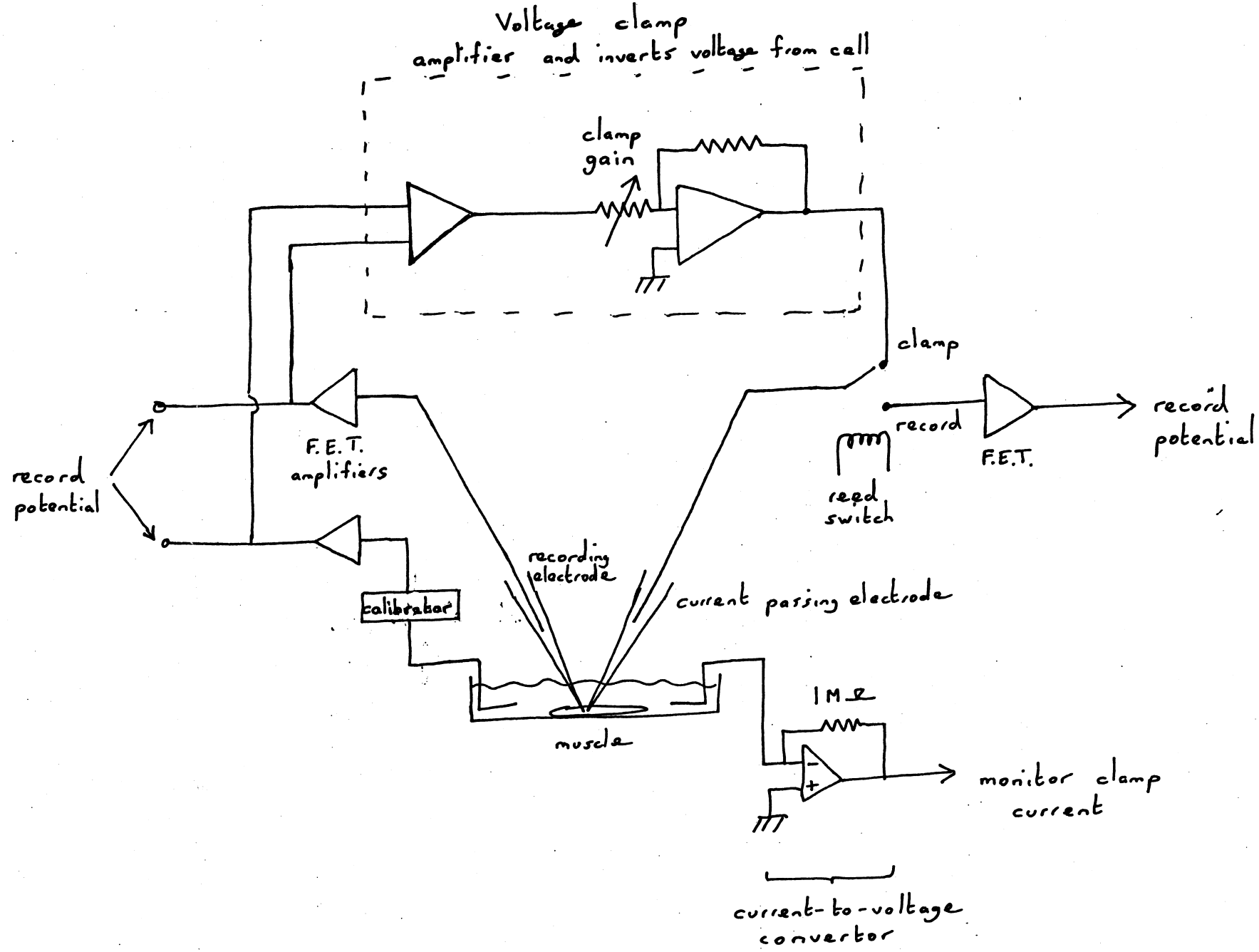

Appendix F
Schematic of voltage clamp

volume. This duration can be significantly extended by lowering the spatial resolution of release and can be significantly reduced by the addition of calcium-buffering agents, whether intrinsic cellular calcium buffers or extrinsic calcium indicator dyes.

There are many possible uses for TPE of calcium cages. The competition of buffers for locally released calcium could provide a window into the spatial heterogeneities of the intrinsic calcium-buffering dynamics in living cells. This could be accomplished through utilization of the relative uptake of liberated calcium ions by a fluorescent calcium indicator and intrinsic calcium buffers as a measure of the intrinsic buffering rate and capacity of cells. As has been shown in Fig. 6, for at least one cell type these kinetics should happen significantly faster than the diffusional escape of calcium ions from the TPE focal volume, allowing these buffering properties to be measured with submicron, three-dimensional resolution and thereby extending previous whole cell studies.[23]

These measurements and calculations demonstrate that complete two-photon release of calcium with high three-dimensional spatial resolution is possible and can be an extremely useful tool in the study of a variety of cellular processes.

Acknowledgments

This work was carried out in the Developmental Resource for Biophysical Imaging and Optoelectronics with funding provided by the NSF (Grant DIR 88002787) and NIH (Grant RR07719 and RR04224). EB was supported as a predoctoral trainee under NIH Grant T32GM08267. Laser excitation at 622 nm was supported by Dr. Frank Wise, Xiang Liu, and Lie-Jia Qian of Cornell University Applied and Engineering Physics.

[21] Caged Inositol 1,4,5-Trisphosphate for Studying Release of Ca^{2+} from Intracellular Stores

By NICK CALLAMARAS and IAN PARKER

Introduction

Inositol 1,4,5-trisphosphate ($InsP_3$) is a second messenger that mediates Ca^{2+} release during many physiological processes, including development, gene regulation, secretion, contraction, synaptic transmission, and apoptotic

0076-6879/98 $25.00

cell death.[1,2] The development of caged-$InsP_3$ [c-$InsP_3$: *myo*-inositol 1,4,5-trisphosphate (1,2-nitrophenyl ester)] has provided an elegant and efficient means by which to control levels of this active messenger in the cytoplasm of intact cells, giving an unparalleled degree of temporal and spatial resolution for detailed studies of this ubiquitous intracellular pathway.[3–5] In comparison to other techniques, such as fast-flow perfusion of permeabilized cells[6] or direct introduction from a point source via a pressure or iontophoresis microelectrode,[7] it allows rapid (millisecond), spatially defined elevations in $InsP_3$ concentration to be achieved without compromising the organization and biochemical composition of the cytoplasm or disrupting the electrical properties of the cell.

The essence of the technique is first to introduce the physiologically inert c-$InsP_3$ into a cell (e.g., by microinjection or diffusion from a whole cell patch pipette) and allow it to diffuse and equilibrate throughout the cytosol. Subsequent illumination with near-UV light then provides a means to photorelease active $InsP_3$. Major advantages of this technique are: (1) rapid and reproducible millisecond steps in intracellular concentration of $InsP_3$ are achieved; (2) the relative concentration of $InsP_3$ can be precisely regulated by the intensity and duration of illumination; and (3) manipulation of the illumination field allows for homogeneous release of $InsP_3$ throughout spatially defined regions of the cell.

Several practical points further simplify the use of c-$InsP_3$ and extend its utility. The caged precursor is extremely stable in the cytosol, and most cells are exquisitely sensitive to $InsP_3$ (nanomolar range), so that a large "reservoir" of c-$InsP_3$ may be loaded, allowing numerous photolysis flashes to be delivered, each of which consume only a tiny fraction of the total c-$InsP_3$. Also, c-$InsP_3$ is efficiently photolyzed by light with wavelengths <400 nm, thus freeing up the visible spectrum for simultaneous use of long-wavelength indicator dyes to monitor Ca^{2+} liberation induced by $InsP_3$.

This article describes techniques developed in the authors' laboratory for use of c-$InsP_3$ in *Xenopus laevis* oocytes and illustrates some of their applications in studying the $InsP_3/Ca^{2+}$ second messenger pathway. The

[1] M. J. Berridge, *Nature* **361,** 315 (1993).
[2] T. Michikawa, A. Miyawaki, T. Furuichi, and K. Mikoshiba, *Crit. Rev. Neurobiol.* **10,** 39 (1996).
[3] D. C. Ogden, K. Khodakhah, T. D. Carter, P. T. Gray, and T. Capiod, *J. Exp. Biol.* **184,** 105 (1993).
[4] S. S. Wang and G. J. Augustine, *Neuron* **15,** 755 (1995).
[5] I. Parker, *Neuromethods* **20,** 369 (1992).
[6] T. Meyer, T. Wensel, and L. Stryer, *Biochemistry* **29,** 32 (1990).
[7] M. J. Berridge, *Proc. R. Soc. Lond. B* **238,** 235 (1989).

Xenopus oocyte has long been a common cell type for studies of the InsP_3-mediated Ca^{2+} release system due to its enormous size (>1 mm diameter) and simple geometry, which facilitate many experimental procedures. Additional advantages are the ability of the oocyte to express foreign proteins encoded by microinjected mRNA[8] and a lack of other confounding intracellular Ca^{2+} release channels (i.e., ryanodine receptors). The combined advantages of flash-photolysis of c-InsP_3 and the oocyte system have, for example, permitted high-resolution studies of the kinetics of InsP_3 receptor (InsP_3R) gating in an intact cell system,[9] allowed elucidation of the relationship between InsP_3-evoked Ca^{2+} signals and Ca^{2+}-dependent Cl^- membrane current,[10] and facilitated the resolution of "elementary" Ca^{2+} release events underlying global Ca^{2+} signals.[11–13] Moreover, the ability to evoke reproducible InsP_3 signals has aided pharmacological studies of agents affecting this intracellular messenger pathway.[14,15]

Methodology

Photochemistry of c-InsP_3

In the native oocyte, InsP_3 is generated from receptor-mediated breakdown of phosphatidylinositol bisphosphate. InsP_3 then binds to the intracellular InsP_3R to release Ca^{2+} from a subset of the intracellular Ca^{2+} stores and is subsequently metabolized into a bewildering array of other inositol phosphates, some of which retain physiological activity. The flash photolysis of c-InsP_3 avoids the time delays, nonlinearity, and modulation by other messengers associated with ligand-activated InsP_3 generation. This is achieved due to the efficiency of the photochemistry involved in the cleavage of InsP_3 from its protecting nitrophenyl ester group.[16] In brief, the reaction proceeds in two steps: the rapid (nanosecond) absorption of a high energy photon generating active intermediates followed by a slower (millisecond) dark reaction whereby intermediates decay to release InsP_3

[8] R. Miledi, I. Parker, and K. Sumikawa, *in* "Fidia Neuroscience Award Lectures" (J. Smith, ed.), Vol. 3, p. 57. Raven Press, New York, 1989.
[9] I. Parker, Y. Yao, and V. Ilyin, *Biophys. J.* **70,** 222 (1996).
[10] I. Parker and Y. Yao, *Cell Calcium* **15,** 276 (1994).
[11] I. Parker and Y. Yao, *Proc. R. Soc. Lond. B* **246,** 269 (1991).
[12] Y. Yao, J. Choi, and I. Parker, *J. Physiol. (Lond.)* **482,** 533 (1995).
[13] I. Parker, J. Choi, and Y. Yao, *Cell Calcium* **20,** 105 (1996).
[14] I. Parker and I. Ivorra, *J. Physiol. (Lond.)* **433,** 207 (1991).
[15] V. Ilyin and I. Parker, *J. Physiol. (Lond.)* **448,** 339 (1992).
[16] J. W. Walker, J. Feeney, and D. R. Trentham, *Biochemistry* **28,** 3272 (1989).

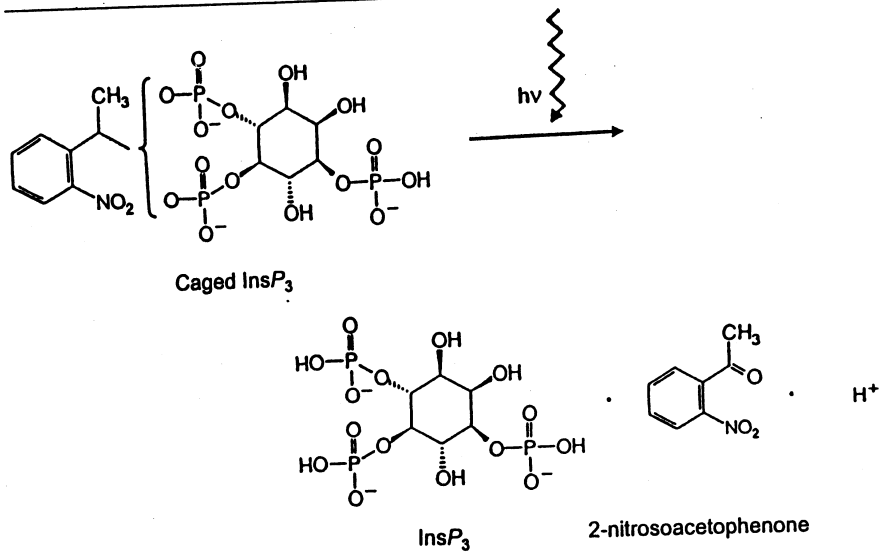

FIG. 1. Schematic photolysis reaction for caged InsP_3. In addition to free InsP_3, photolysis releases a proton and a by-product, 2-nitrosoacetophenone.

(Fig. 1). The by-products of this reaction, a proton and nitrosoacetophenone, can be toxic at high levels (1 $mmol^{-1}$), altering the local pH or reacting with -SH groups of proteins, respectively.[17] Fortunately, the concentrations of InsP_3 necessary to elicit even maximal responses in oocytes and many other cells are sufficiently small that by-product toxicity appears not to be an issue.

Caged InsP_3 can presently be obtained from either Calbiochem (La Jolla, CA) or Molecular Probes (Eugene, OR). In our experience the c-InsP_3 available from Molecular Probes is preferable because of lower contamination by active InsP_3.

Introduction of c-InsP_3 into Cells

Caged InsP_3 is a highly charged molecule and thus does not permeate through the cell membrane. For work with single cells, c-InsP_3 may be introduced into the cytosol by injection through a micropipette (pneumatic presure injection or ionophoresis) or by diffusion from a whole cell patch pipette. In the latter case, the resulting intracellular concentration should approximate that in the pipette. Pressure injection is convenient for use with large cells, and the final intracellular concentration of c-InsP_3 can be

[17] M. G. Hibberd, Y. E. Goldman, and D. R. Trentham, *Curr. Topics Cell. Regul.* **24,** 357 (1984).

estimated from the amount of fluid injected (measured as the diameter of a fluid droplet expelled with the pipette tip in air), the concentration in the injection solution, and the cytosolic volume.

Injection into defolliculated *Xenopus* oocytes[18] is made through broken (tip diameter ca. 5 μm) glass micropipettes. We typically inject about 20 nl of an aqueous solution of 1–5 m*M* c-InsP_3 (to which Ca^{2+} indicator dyes may also be added), resulting in a final intracellular concentration of about 20–100 μM, assuming a cytosolic volume of 1 μl. It is then necessary to wait for 30 min or longer for diffusional equilibration of c-InsP_3 throughout the cell; this time also allows the cell to metabolize any active free InsP_3 that may be present as a contaminant.[5] Standard room lights, and even halogen fiber-optic illuminators, cause surprisingly little photolysis of c-InsP_3, and we have not found it necessary to take any special precautions with lighting either in handling injection solutions or after loading cells with c-InsP_3.

Clearly, mechanical introduction of c-InsP_3 through pipettes would be impractical for studies on populations of cells. An elegant approach that has recently been developed involves loading c-InsP_3 by extracellular application at a membrane-permeable ester,[19] analogous to the well-known technique for loading indicators such as Fura-2. Alternatively, the plasma membrane may be permeabilized by a variety of techniques[20] to allow access of charged c-InsP_3 to the cytosol.

Linearity and Calibration of Photorelease

The amount of free InsP_3 resulting from a given photolysis flash is expected to be linearly proportional to the starting concentration of c-InsP_3 and the flash intensity and duration. In practice, this linear dependence on flash parameters is followed almost exactly; as illustrated in Fig. 2A, where caged ATP was used to monitor photolysis in place of c-InsP_3 because of the ease of detecting release of ATP by luminescence of a luciferin/luciferase assay system. Thus, an extremely precise control of *relative* amounts of InsP_3 formation within a given cell can be obtained by appropriate adjustment of flash parameters. Our usual method is to adjust the flash intensity using neutral density filters to set an initial working range and then vary the flash duration to control the extent of photorelease. This has advantages in that the duration can be readily altered in very small increments, as opposed to the relatively coarse steps available with filter

[18] K. Sumikawa, I. Parker, and R. Miledi, *Methods Neurosci.* **1**, 30 (1989).
[19] W. H. Li, C. Schultz, J. Lopi, and R. Y. Tsien, *Tetrahedron* **53**, 12017 (1997).
[20] K. A. Oldershaw, D. L. Nunn, and C. W. Taylor, *Biochem. J.* **278**, 705 (1991).

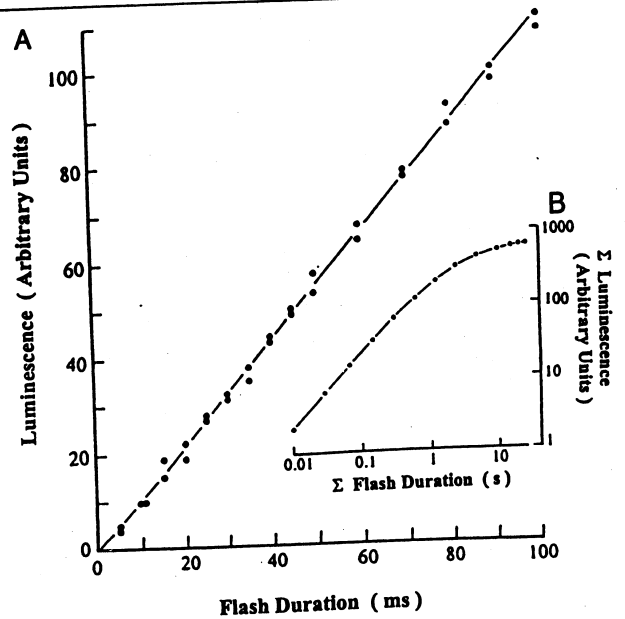

FIG. 2. Linearity of photorelease with flash strength and calibration of extent of photolysis using a luminescence system to assay release of ATP from a caged precursor. (A) Formation of ATP varies linearly with flash duration. Recordings were made from a 20-μl droplet containing 100 μM caged ATP together with undiluted ATP assay reagent (Sigma FL-AAM). The photolysis light was focused by the microscope objective to a small spot within the droplet, and the graph plots the peak amplitude of the ATP-dependent luminescence (monitored by a photomultiplier) evoked following photolysis flashes of identical intensity and varying duration. (B) Estimation of the fractional photolysis of caged ATP resulting from a given photolysis flash. The experiment was performed as in (A), except for use of a smaller droplet that was entirely irradiated by the photolysis spot. A series of repeated flashes of increasing duration were applied, and the peak luminescence recorded following each flash. Double logarithmic plot shows cumulative luminescence (i.e., sum of peak signals evoked by successive flashes) as a function of cumulative duration of exposure to photolysis light. [Reproduced from I. Parker and I. Ivorra, *Am. J. Physiol.* **263**, C154 (1992), with permission.

wheels, and individual flashes within a paired-pulse protocol can be independently controlled. Care should be taken, however, that the longest flashes employed are brief compared to the kinetics of the response under investigation.

For many purposes, control of the *relative* amounts of InsP_3 photoreleased in a given experiment is sufficient, but it may also be necessary to estimate the *absolute* concentrations of free InsP_3. This is a more difficult and less precise task, for which we have taken two approaches. The first

involves an *in vitro* calibration employing caged ATP.[21] The protocol is illustrated in Fig. 2B. A small droplet containing a known amount of ATP together with assay mixture is placed on the microscope stage and is completely irradiated by photolysis flashes of the same intensities as used for physiological experiments. Repeated flashes are applied, and the luminescence signals (linearly proportional to the amount of ATP) are recorded following each flash. After many exposures, the luminescence response declines to zero, indicating complete consumption of the c-ATP (luciferin is present in excess). Thus, the total cumulative luminescence over all responses corresponds to the photorelease of all the ATP, and the fractional amount released by a given light flash can be calculated from the ratio of the luminescence resulting from that flash compared with the total luminescence. This fractional release should then apply equally to photolysis of intracellular c-InsP_3 under the same conditions, with the major caveat that no account is taken of light absorption within the specimen. A second approach is to employ the cell as a bioassay system. In the oocyte, Ca^{2+} waves are initiated at a sharply defined concentration of InsP_3 so that photolysis flashes below threshold evoke little or no Ca^{2+} release or Ca^{2+}-dependent Cl^- current response, whereas just-suprathreshold stimuli give clear responses (cf. Fig. 4). Estimates of the absolute concentration of InsP_3 corresponding to this threshold can then be obtained by injecting increasing amounts of a poorly metabolized but equipotent InsP_3 analog (3-F-InsP_3) to determine the resulting intracellular concentration at which waves are triggered.[12]

Measurements of the InsP_3 concentrations by both of these methods indicate that Ca^{2+} waves are evoked in the oocyte by roughly 50 nM InsP_3, and maximal responses are evoked by concentrations about 20-fold greater.[9] Because the cells can readily be loaded to concentrations of c-InsP_3 as high as 100 μM, flashes giving physiological responses will photolyze only negligible proportions (0.05–1%) of the c-InsP_3. Further, the turbidity of the oocyte cytoplasm limits light penetration to a few tens of μm, so that the greater volume of the cell is effectively shielded from the photolysis light and acts as a virtually inexhaustible reservoir of fresh c-InsP_3. The net result is that it is possible to evoke numerous (hundreds) reproducible responses with repeated flashes, without significant depletion of available c-InsP_3 in the oocyte.

Photolysis Light Sources

The photolysis of caged InsP_3 requires a sufficiently intense source of illumination at wavelengths around 350 nm. Possible light sources capable

[21] I. Parker and I. Ivorra, *Am. J. Physiol.* **263,** C154 (1992).

of efficient photolysis in most biological preparations include (1) continuous arc lamps with electronically controlled shutters, (2) xenon flash lamps, and (3) UV lasers. The preceding systems are ordered in terms of increasing energy, complexity, and cost. Each system has relative merits and disadvantages but, fortunately, bigger and costlier systems are not necessarily better.

A continuous UV arc lamp is a stable source of illumination that, when combined with commercially available high-speed electric shutters, provides an inexpensive and highly efficient photolysis system. The stability of the lamp output is very good if the arc is mounted vertically and powered from a high-quality constant current power supply, with a between-flash reproducibility of better than 1%. For use with caged-InsP_3, the limited power of the lamp is not a major consideration because photolysis of only a small percentage of the c-InsP_3 loaded into a cell is sufficient to evoke responses. Either mercury or xenon arc lamps (50–100 W) work well and, indeed, it is usually necessary to attenute their output with neutral density filters. High-speed electronically controlled shutters provide an affordable and efficient means to produce flashes as brief as 1–2 msec. Durations shorter than this would provide little advantage because the photogeneration of InsP_3 from its caged precursor takes 5–10 msec. Finally, unlike flash lamps or pulsed lasers, it is possible to continuously irradiate the specimen, mimicking physiological InsP_3 generation over several seconds during agonist stimulation. Therefore, a continuous arc lamp is the simplest and most cost-effective choice for most experimental situations. Such systems can be readily constructed from an existing epifluorescence microscope, merely by substituting a UV filter cube to restrict irradiation to wavelengths <400 nm and inserting an electronic shutter into the light path.

Xenon flash lamps[22] provide a much higher (1000 times or greater) energy output in a brief flash than a shuttered arc lamp system but, as noted earlier, this higher energy is not likely to be required when working with c-InsP_3 provided that an efficient optical system is used to channel light to the specimen. Further, flash lamp systems have disadvantages in regard to their greater cost, generation of electrical artifacts, lack of independent control of the duration of each flash in paired-pulse experiments, and an inability to provide continuous illumination of sustained photorelease.

Several types of laser are available that produce high-energy pulses at near-UV wavelengths, including the frequency-doubled ruby laser and the frequency-tripled Nd–YAG (neodymium–ytrrium-aluminum-garnet) laser. In our experience, the only application for which the high cost of these lasers is justified involves focusing the photolysis light to a near-diffraction limited spot in the specimen so as to achieve a virtual point-photorelease

[22] G. Rapp and K. Guth, *Pflugers Arch.* **411,** 200 (1988).

of InsP_3. Because of the perfectly parallel beam from a laser this can be achieved with little loss of light, whereas to achieve the same result with a conventional (arc lamp) source involves insertion of a pinhole aperture with an accompanying drastic loss in light throughput.

Two-photon excitation of caged compounds by femtosecond pulses from mode-locked lasers is a recent development[23] that offers the possibility of even more spatially restricted photorelease because the quadratic dependence of two-photon photolysis on light intensity ensures that this will be restricted only to the plane of focus of the light spot formed by an objective lens. Although this approach has been elegantly employed to map out the sensitivity of neurons to extracellular photorelease of caged neurotransmitter,[24] the possible advantages of this expensive technology for use with c-InsP_3 are unclear and are likely to be limited by the physiology of the InsP_3 pathway. In particular, the rapid intracellular diffusion of InsP_3, together with the long latencies (many milliseconds) before Ca^{2+} release begins, suggests that the spatial localization of InsP_3 will be limited by those factors and not by the minimum volume throughout which photorelease occurs.

Simultaneous Use of c-InsP_3 and Fluorescent Calcium Indicators

The primary action of InsP_3 in the cell is to liberate calcium from intracellular stores. One approach to monitor the resulting rise in cytosolic-free calcium concentration is to measure currents through endogenous calcium-activated membrane channels (e.g., the Ca^{2+}-dependent Cl^- channels in the oocyte membrane.[25] This is advantageous in terms of simplicity and ensures that the measurement technique does not perturb the signals of interest. Interpretation may, however, be complicated by uncertainties regarding the steady-state and kinetic relationships between free [Ca^{2+}] and current amplitude,[10] and voltage-clamp recordings of current provide no information regarding the spatial distribution of calcium within the cell. Thus, for many purposes it is desirable to have a more direct measure of cytosolic calcium. The availability of a wide range of fluorescent calcium indicator dyes operating in the visible spectrum makes it possible to combine fluorescence calcium monitoring or imaging together with simultaneous photolysis of ç-InsP_3.

Currently, our favorite dyes are the Oregon green family (Molecular Probes), which are optimized for excitation by the 488-nm line of the argon ion laser and fluoresce in the green. The excitation spectra of these dyes are sufficiently separated from that of c-InsP_3 that we find little practical

[23] W. Denk and K. Svoboda, *Neuron* **18,** 351 (1997).
[24] W. Denk, *Proc. Natl. Acad. Sci. U.S.A.* **91,** 6629 (1994).
[25] R. Miledi and I. Parker, *J. Physiol. (Lond.)* **357,** 173 (1984).

difficulty with photolysis of c-InsP_3 resulting from the blue excitation light and, conversely, photolysis flashes at wavelengths <400 nm cause little or no artifacts in fluorescence recordings. Furthermore, the dyes are available as variants with different calcium affinities (e.g., Oregon green 488 BAPTA-1 has an affinity of a few hundred nanomolar, and Oregon green BAPTA-5N has a low affinity of a few tens of micromolar), so that they may be used selectively to examine small calcium signals close to the basal calcium level or large calcium transients evoked by maximal InsP_3 levels. A disadvantage of all currently available long-wavelength indicators is that, unlike the UV-excited dyes Fura-2 and Indo-1, none show shifts in either excitation or emission spectra on binding calcium. Thus, using a single dye, it is not possible to ratio signals at two wavelengths to obtain a calibration of free calcium levels independent of variations in dye loading and path length. A reasonable compromise, however, is to form a "pseudo ratio" signal by expressing calcium-dependent fluorescence signals relative to the resting fluorescence before stimulation.[2]

The basic principle in designing an optical system for simultaneous fluorescence monitoring and photolysis is to "stack" dichroic mirrors so as to split off appropriate parts of the visible and UV spectra. Thus, a UV dichroic mirror placed close to the microscope objective will reflect short wavelengths (<400 nm) from a photolysis light source onto the specimen but transmit longer wavelengths, which may then be further split by an additional dichroic mirror to separate fluorescence excitation and emission wavelengths appropriate for specific dyes. In our earlier optical system[5] employing a Zeiss Universal microscope, this "stacking" was possible by physically mounting one epifluorescence attachment on top of another. More modern microscope designs fail to anticipate the need for such flexibility, and in our present system (described in the following section) a UV dichroic mirror is placed in the regular epifluorescence unit, whereas the fluorescence excitation dichroic mirror is located externally to the microscope with light directed through the video port. Excellent dichroic mirror and filter sets tailored for use with particular dyes are available from Omega Optical Inc. and Chroma Technology Corp. (both at Brattleboro, VT).

Fluorescence calcium monitoring systems may vary in their degree of spatial and temporal resolution (with corresponding increases in cost and complexity) from photomultiplier-based detectors to monitor calcium throughout an entire cell or defined region of a cell,[5] through CCD camera-based wide-field imaging systems[11] to laser-scan confocal microscopes providing millisecond and submicron resolution.[26]

[26] I. Parker, N. Callamaras, and W. Wier, *Cell Calcium* **21,** 441 (1997).

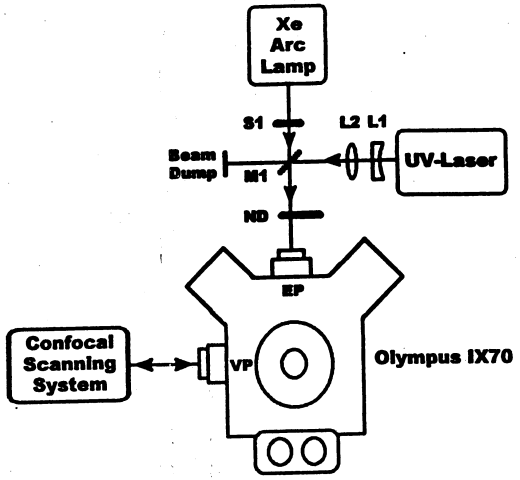

FIG. 3. Schematic diagram of a versatile photolysis and imaging system constructed around an Olympus IX70 inverted microscope. The photolysis system is shown at the top, and interfaces through the epifluorescence port (EP) of the microscope. A confocal scanning system on the left interfaces through the video side port (VP). L1, plano-concave lens; f, −1 cm; L2, biconvex lens; f, 5 cm; S1, electronic shutter; M1, cover glass acting as beam splitter; ND, neutral density filter wheels.

Versatile Photolysis System for Imaging and Electrophysiological Studies

This section describes details of our current photolysis system, which operates through the epifluorescence port of an Olympus IX70 inverted microscope (Lake Success, NY), and can be used either independently or together with a confocal Ca^{2+} imaging system interfaced through the microscope video port (Fig. 3). For further details of the confocal scanner, see Parker *et al.*,[26] and for more general information pertaining to the principles and applications of biological confocal microscopy, see Pawley.[27]

The photolysis system employs both a continuous arc lamp source (for wide field photorelease) and a pulsed UV laser (for "point" photorelease), with light from both systems being combined by a beam-splitting mirror and directed into the epifluorescence port of the Olympus IX70, which is equipped with a standard UV filter cube and fluor objective lenses. Components are mounted on an optical breadboard, using standard post-mounts (New Focus Inc., Santa Clara, CA). Note that with the exception of the filter cube and holder, no Olympus epifluorescence components are required.

The upper section of Fig. 3 shows the layout of the photolysis light

[27] J. B. Pawley, "Handbook of Biological and Confocal Microscopy." Plenum Press, New York, 1990.

paths. All lenses are fused silica for optimal UV transmission, and optical components are postmounted at a height corresponding to the center line of the Olympus epifluorescence port. For experiments where photorelease of caged compound is required over a wide area (10- to 100-μm-diameter spot using a 40× objective), UV light is derived from an arc lamp (75-W xenon lamp, mounted in a Zeiss housing and operated from a stabilized constant-current power supply). An electronic shutter (Uniblitz, Vincent Associates, NY), triggered manually or via TTL input from a Digitimer or computer, controls exposure duration while a set of neutral density wheels (3.0 OD in steps of 0.1 OD, New Focus Inc.) allow control of light intensity. Adjustment of a collector lens in the arc lamp housing provides uniform (Koehler) illumination throughout the photolysis spot in the microscope image plane.

The laser system employs a Mini-Lite frequency-tripled (355 nm) Nd:YAG laser (Continuum, Santa Clara, CA), with the laser head mounted on the optical table by nylon screws and insulating stand-offs to avoid hum loops for electrophysiological recording. Lenses L1 and L2 form a beam expander so that the laser beam fills the back aperture of the objective lens, thus making use of its full numerical aperture. Because the laser beam at full power may crack an objective lens with poor UV transmission, a microscope cover glass is used as a mirror (M4) to reflect only a small percentage of the laser beam into the microscope through the neutral density filter wheels, which allow further attenuation. The invisible beam from the Mini-Lite presents a considerable safety hazard, and appropriate precautions, including use of laser safety goggles, should be taken when the beam is exposed for alignment. A beam dump is placed after M4 to avoid the possibility of the beam passing into the room, and the entire beam path is covered while the laser is operating. The laser spot formed by an objective lens can be viewed using a coverslip marked with a yellow "highlighter" pen, and its position centered by small adjustments of laser position and deflection of M1. Finally, the spot can be brought to a sharp focus by axial adjustment of L2. A UV-blocking filter in the Olympus filter cube, together with an additional long-pass filter (λ >510 nm) inserted in the microscope binocular head, permits safe viewing while the laser is in use. The laser can be operated in single-shot mode (triggered by a push switch or TTL input) or pulsed repeatedly at up to 10 Hz.

Applications of c-$InsP_3$ for Study of Ca^{2+} Signaling in Oocytes

Dose–Response Relation of Ca^{2+} Release

Bath application of calcium-mobilizing agonists to oocytes results in a complex oscillatory Cl^- current, which varies in a highly nonlinear manner

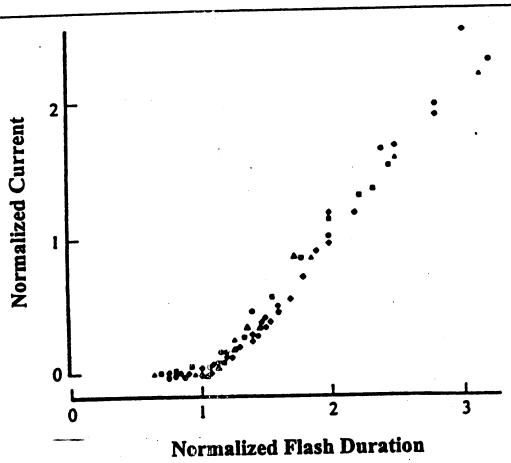

FIG. 4. Dose–response relationship of membrane currents evoked by photorelease of InsP_3 by different durations of irradiation. Pooled data from five oocytes (indicated by different symbols) showing the relationship between flash duration and peak size of evoked currents. Flash durations are normalized with respect to that which evoked just-suprathreshold responses in each oocyte, and currents are normalized with respect to currents evoked in each oocyte evoked by a flash of twice threshold duration. In this experiment the entire vegetal hemispheres were exposed to UV light. [Reproduced from I. Parker and I. Ivorra, *Am. J. Physiol.* **263,** C154 (1992), with permission.]

with agonist concentration.[28] The intracellular location of the numerous stages in the signaling pathway between cell surface receptors and activation of the current, however, makes it difficult to determine at which stage the nonlinearity arises. Photolysis of caged InsP_3 offers an elegant means to circumvent this problem bypassing earlier stages in the pathway. Indeed, the reproducibility and linearity of photolysis allow intracellular dose–response relationships to be determined with the same ease as bath application of compounds to an extracellular receptor. For example, Fig. 4 illustrates the dependence of Ca^{2+}-activated membrane currents on the strength of photolysis flashes and demonstrates a nonlinear relationship in that a threshold amount of InsP_3 is needed before any current is generated. These data also illustrate the reproducibility of the photolysis technique, as evident in the close overlap of measurements from five oocytes when flash strengths are normalized relative to the threshold required to evoke a detectable current in each cell so as to compensate for differing amounts of microinjected c-InsP_3.

[28] I. Parker, K. Sumikawa, and R. Miledi, *Proc. R. Soc. Lond. B.* **231,** 37 (1987).

Pharmacological Studies of InsP_3R in Intact Oocytes

The InsP_3R through which calcium liberation occurs is a potential site for modulation by many endogenous messenger compounds and exogenous pharmacological agents. Studies of such effects on calcium mobilization are complicated, however, if extracellular agonists are used to activate the InsP_3 pathway because different agents may act on stages between the cell surface receptor and InsP_3 formation, as well as on the InsP_3R itself. Again, caged InsP_3 provides a means to circumvent these difficulties by allowing the effects of microinjected or (for membrane-permeant substances) bath-applied agents to be monitored on signals evoked by repeated and identical pulses of intracellular InsP_3. Two examples are shown in Fig. 5.

The first concerns the possible physiological roles of Ins(1,3,4,5)P_4 (InsP_4), a higher-order inositol polyphosphate that is formed transiently by phosphorylation of InsP_3 during activation of the signaling pathway. As shown in Fig. 5A, evidence that InsP_4 acts as a weak agonist at the InsP_3R to potentiate calcium mobilization is obtained by microinjecting InsP_3 into oocytes while monitoring calcium-dependent Cl^- currents evoked by InsP_3 photoreleased by successive, just-suprathreshold flashes.[14] A strong potentiation of the currents is observed, even with small doses of InsP_4 which, themselves, evoke almost detectable responses. This experiment further illustrates a technical point, in that it is necessary to microinject the highly charged InsP_4 into the oocyte. The spatial spread of InsP_4 in the cell is restricted to a region around the pipette tip because of diffusion and metabolism, and the photolysis light is therefore focused as a small spot centered around the injection pipette. Even though voltage-clamp recordings reflect current from the whole membrane area of the oocyte, the evoked Cl^- currents thereby arise only from the local region exposed to InsP_4.

A second example of the use of c-InsP_3 for pharmacological studies concerns the actions of caffeine, which is widely used as a tool to discriminate between calcium mobilization mediated through InsP_3R and ryanodine receptors, by virtue of its ability to potentiate ryanodine receptor-mediated responses. Because caffeine readily permeates the cell membrane, we were able to study its actions on InsP_3-evoked Cl^- current responses by bath application during trains of repetitive photolysis flashes.[29] This causes a dramatic and reversible reduction in responses (Fig. 5B) and a rightward shift in the dose–response curve for InsP_3 (Fig. 5C), suggesting that caffeine may act as a reversible antagonist at the InsP_3 receptor. In this and other experiments where calcium liberation is monitored by endogenous calcium-

[29] I. Parker and I. Ivorra, *J. Physiol.* (*Lond.*) **433,** 229 (1991).

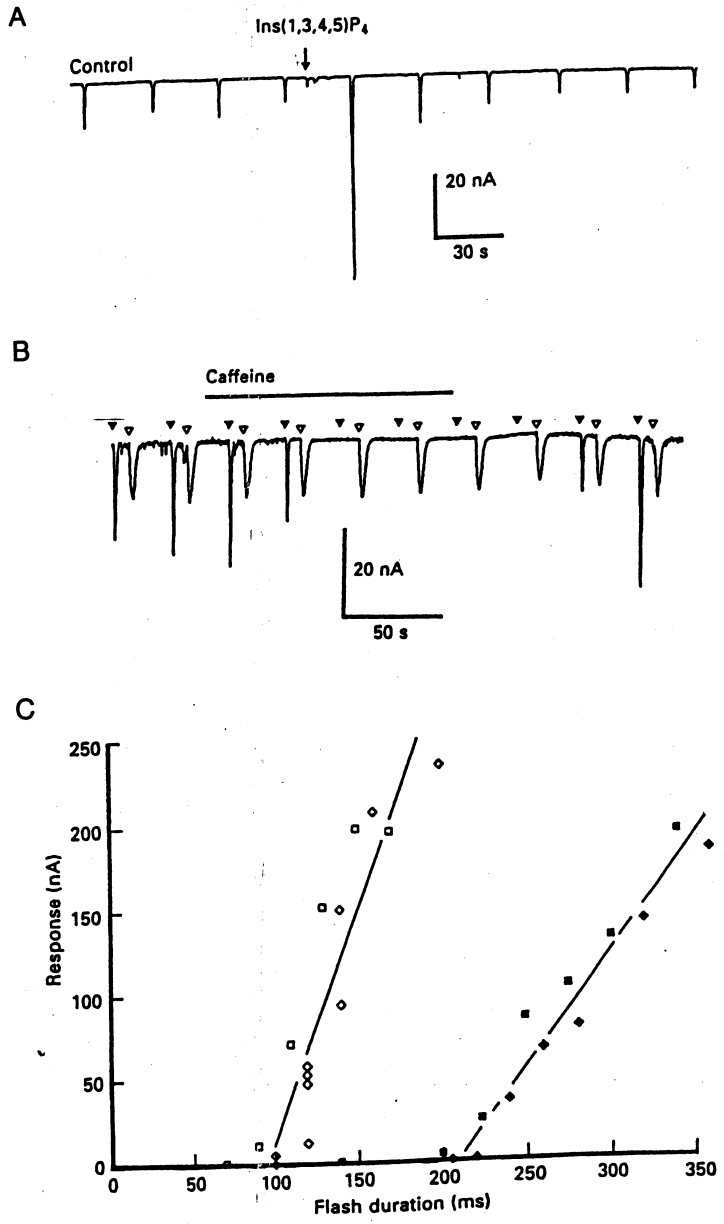

FIG. 5. Utility of c-InsP_3 for pharmacological studies. (A) Responses evoked by photorelease of InsP_3 are facilitated by injection of low doses of InsP_4. Trace shows calcium-dependent membrane current responses (inward currents at a clamp potential of −60 mV) evoked by repetitive, identical photolysis flashes, with a duration just above the threshold to evoke detectable signals. InsP_4 (about 1 fmol) was injected into the oocyte when marked by the arrow. [Reproduced from I. Parker and I. Ivorra, *J. Physiol. (Lond.)* **433**, 207 (1991), with permission of the Physiological Society.] (B) Bath-applied caffeine inhibits InsP_3-evoked membrane current responses, but not the activation of the Ca^{2+}-dependent Cl^- current. Trace shows currents evoked by alternate stimulation by photolysis flashes (filled arrowheads) and intracellular injections of calcium (open arrowheads). Caffeine (5 m*M*) was bath-applied when marked by the bar. (C) Caffeine increases the threshold amount of InsP_3 required to evoke membrane currents. Graph shows amplitudes of currents evoked by photolysis flashes of varying durations in the absence (open symbols) and presence (filled symbols) of 2.5 m*M* caffeine. [B, C reproduced from I. Parker and I. Ivorra, *J. Physiol. (Lond.)* **433**, 229 (1991) with permission of the Physiological Society.]

activated currents it is, however, important to countrol for possible effects on the calcium-activated Cl^{-1} channels themselves. Monitoring of intracellular calcium by means of indicator dyes is one obvious approach, but in the experiment shown in Fig. 5B, intracellular injections of calcium through a micropipette are interspersed with photolysis flashes to directly activate Cl^- currents and serve as a control.

Temporal Control and Kinetics of the Release Process

The photorelease of InsP_3 is rapid (a few milliseconds) following a photolysis flash, so that the kinetics of calcium liberation in response to a virtually instantaneous step of InsP_3 concentration can be studied. Furthermore, photolysis by a broad light spot results in a homogeneous release of InsP_3 throughout a volume of the cell, thus obviating problems of diffusion delays that arise in other techniques such as intracellular microinjection or extracellular applications of InsP_3 to permeabilized cells. An example is shown in Fig. 6, where a laser confocal microscope is used to monitor calcium fluorescence signals from a minute volume within the oocyte (ca. 1 fl) in response to InsP_3 photoreleased throughout a larger region of the cell surrounding the laser spot. Calcium signals following photolysis flashes of increasing strength begin with progressively shorter latencies and show increasing rates of rise (Fig. 6A). Because the fluorescence signal reflects accumulation of calcium in the cytosol, differentiation of the signal further provides a measure of the rate of calcium efflux (Fig. 6B), allowing a more detailed study of the dependence of the kinetics of opening of the release channels on the concentration of InsP_3.[9]

As is evident in Fig. 6B, calcium liberation following a photolysis flash terminates within a few hundred milliseconds, even though the levels of InsP_3 remain elevated for several seconds.[21] Thus, the InsP_3R enters a refractory state from which its subsequent recovery can be investigated by applying paired photolysis flashes at varying intervals, in a manner analo-

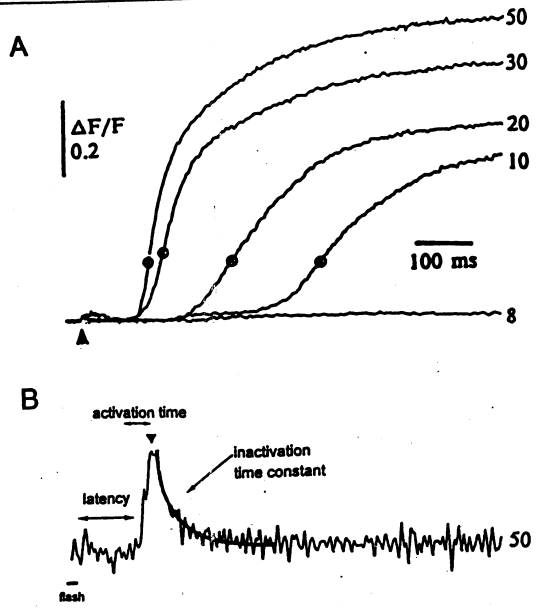

FIG. 6. Calcium transients and kinetics of calcium liberation in response to photorelease of varying amounts of InsP_3. (A) Superimposed fluorescent signals evoked by light flashes of varying durations (indicated in milliseconds at the right of each trace). The arrowhead indicates the time of the flash and circles indicate the point of maximal rate of rise of the signal. The oocyte was loaded with the low-affinity indicator calcium green-5N, together with c-InsP_3. (B) The time differential [$d(\Delta F/F)/dt$] of the 50-msec trace from (A), indicating the kinetics of Ca^{2+} flux. [Modified from I. Parker, Y. Yao, and V. Ilyin, *Biophys. J.* **70,** 222 (1996), with permission of the Biophysical Society.]

gous to the paired-pulse experiments used to examine the refractory state of voltage-gated channels.[30,31] The onset and recovery from inactivation are determined by delivering paired, identical photolysis flashes at varying intervals and monitoring the calcium-activated currents evoked by the second flash in each pair relative to that evoked by a single flash (Fig. 7). At short intervals the calcium signal is potentiated by a preceding flash, but becomes almost completely suppressed as the interval is lengthened to about 2 sec, and subsequently recovers over several seconds.

Entry into and recovery from the refractory state undoubtedly have an important role in generation of the repetitive calcium spikes observed in various cells during sustained activation by extracellular agonists.[32] A characteristic feature is that the frequency of spiking increases with agonist

[30] I. Parker and I. Ivorra, *Proc. Natl. Acad. Sci. U.S.A.* **87,** 260 (1990).
[31] V. Ilyin and I. Parker, *J. Physiol.* (*Lond.*) **477,** 503 (1994).
[32] M. J. Berridge and A. Galione, *FASEB J.* **2,** 3074 (1988).

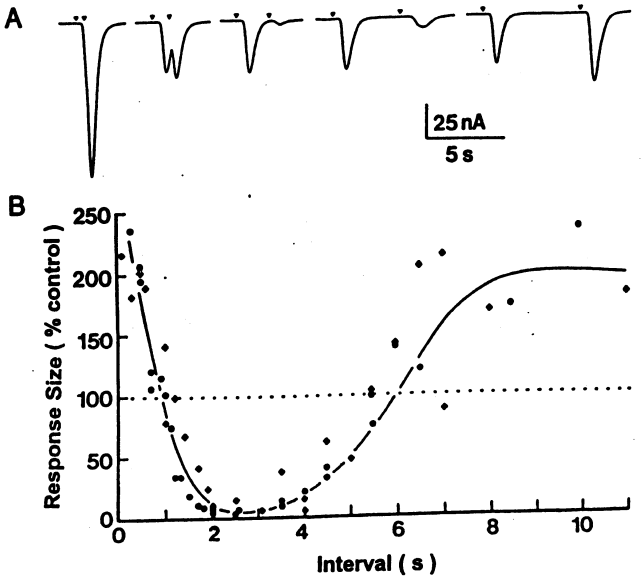

FIG. 7. Paired-flash experiment to investigate the onset and recovery of InsP_3-mediated calcium release. (A) Examples of membrane currents evoked by paired, identical flashes delivered at different intervals. Arrowheads mark the times of each flash. (B) Size of the response to the second flash plotted against interval between flashes. Data are shown from two oocytes (different symbols) and are scaled as a percentage of the response evoked by a single flash. [Reproduced from I. Parker and I. Ivorra, *Proc. Natl. Acad. Sci. U.S.A.* **87,** 260 (1990), with permission.]

concentration but, as noted before, interpretation of these findings is complicated by the complex stages in the messenger pathway between the cell surface receptor and the generation of InsP_3. An alternative approach is to use sustained illumination with low-intensity UV light to cause a prolonged elevation of intracellular [InsP_3] to levels proportional to the light intensity.[33] This results in repetitive spikes in the fluorescence calcium signal during the period of photolysis, which increase in frequency with increasing photorelease but become smaller and superimposed upon a more sustained calcium elevation (Fig. 8).

Spatial Control and Heterogeneity of Calcium Release Sites

The use of light as a stimulus to evoke photolysis of c-InsP_3 permits not only control of the magnitude and kinetics of InsP_3 formation, but also control of its spatial distribution. Thus, information can be obtained

[33] I. Parker and I. Ivorra, *J. Physiol.* (*Lond.*) **461,** 133 (1993).

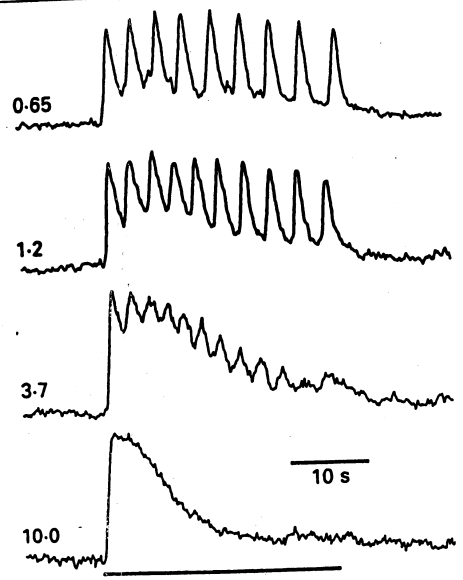

FIG. 8. Repetitive Ca^{2+} spikes during prolonged photorelease of InsP_3. Tracaes show point-confocal Ca^{2+} signals (rhod-2 fluorescence) evoked at a single recording spot by various intensities of photolysis light. Horizontal bar indicates the duration of exposure, and numbers next to each trace indicate the intensity of illumination as a percentage of maximum. [Reproduced from I. Parker and I. Ivorra, *J. Physiol.* (*Lond.*) **461**, 133 (1993), with permission of the Physiological Society.]

regarding the spatial aspects of subcellular calcium liberation, either by restricting photolysis to defined regions of the cell or by fluorescence imaging of the patterns of calcium liberation evoked by spatially homogeneous photolysis. The following examples illustrate use of these approaches to study calcium liberation at increasingly fine levels of resolution, from global signals involving the whole cell to elementary calcium events located to within a few microns.

Figure 9 illustrates an experiment in which the regional sensitivity to InsP_3 is mapped across the two hemispheres (animal and vegetal) of the polarized oocyte cell. The oocyte was loaded with caged InsP_3 and stimulated by identical light flashes focused as a 50 × 50-μm square. As the photolysis square is moved from the vegetal to the animal pole, the whole-cell Cl^- currents evoked by the flashes grow progressively larger (Fig. 9A), indicating increased sensitivity to InsP_3. Thus, even though the voltage-clamp recording summates membrane currents from the whole cell, spatial information is provided by the localized photorelease of InsP_3. One complication in such experiments, however, is that the extent of photorelease may

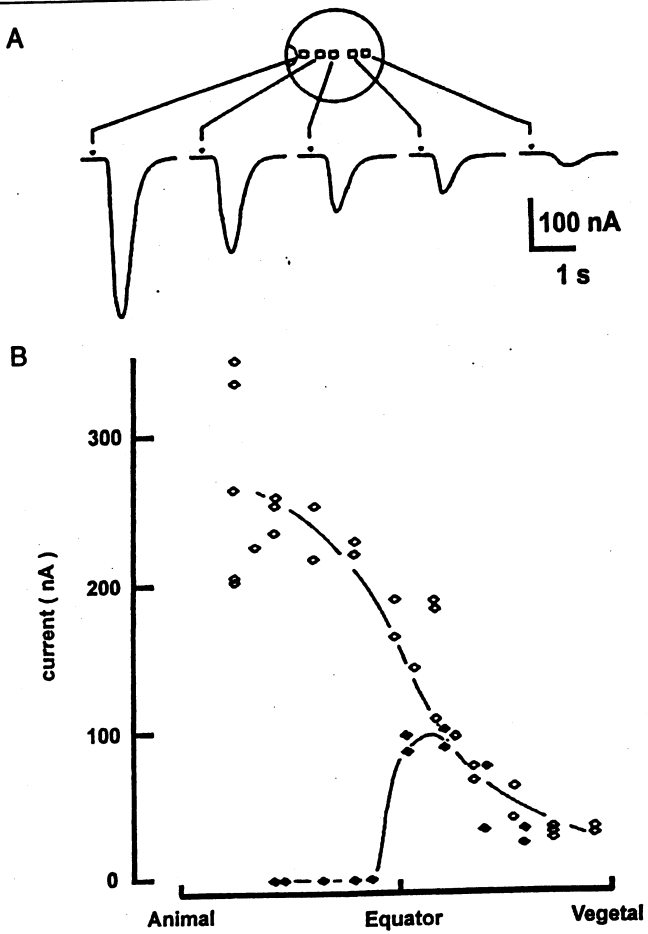

FIG. 9. Spatial variation in currents evoked by InsP_3 photoreleased at different locations across the animal/vegetal axis of the oocyte. (A) Traces show currents evoked by identical light flashes, with the photolysis light focused as a small square at different locations on the albino oocyte as denoted in the diagram. The oocyte was oriented with the germinal vesicle (animal pole) to the left. (B) Variation in the peak size of the current at different photolysis positions. Filled symbols are measurements from a pigmented oocyte and open symbols from an albino oocyte. Curves were drawn by eye.

be affected by optical factors in the cell. Wild-type oocytes are strongly pigmented in the animal hemisphere. In these cells, sensitivity to photolysis flashes is greatly reduced in the animal hemisphere (filled symbols, Fig. 9B), presumably because the superficial pigment blocks penetration of photolysis light into the cell. In the experiment illustrated (Fig. 9A and

open symbols Fig. 9B), this problem was avoided by use of oocytes from albino frogs, which lack pigmentation.

To examine heterogeneity in sensitivity between different functional calcium release sites at a finer (micrometer) scale,[13] the UV light was focused to a spot of about 2 μm diameter by a pinhole aperture placed in the arc lamp photolysis system, and fluorescence calcium signals were monitored by a confocal laser spot concentric with the photolysis spot (Fig. 10). Calcium liberation at this localized level shows an all-or-none

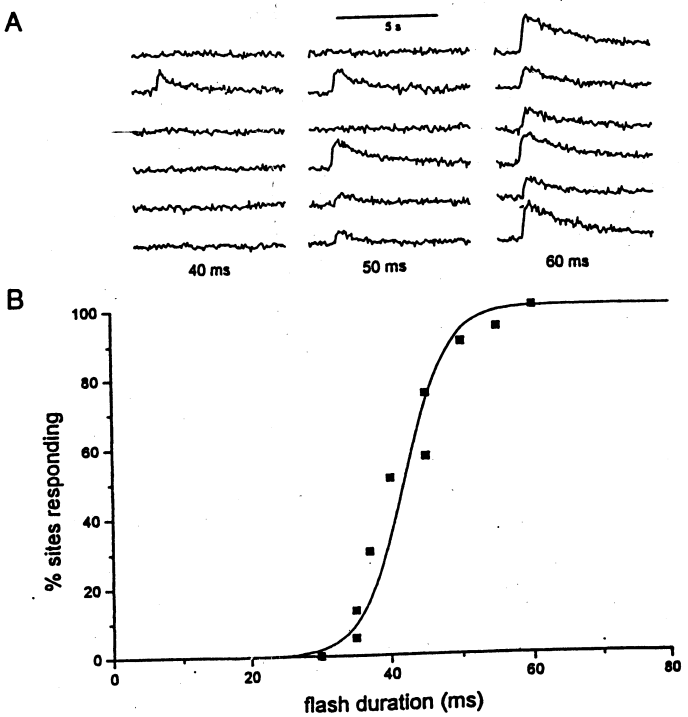

FIG. 10. Local pinhole photorelease of InsP_3 reveals little variation in sensitivity to InsP_3 at different sites. (A) Traces show Ca^{2+} fluorescence monitored from a stationary confocal spot in response to photorelease of InsP_3 evoked by flashes of UV light focused to a 2-μm spot concentric with the confocal spot. Each trace was obtained with the oocyte moved to a new random position, and the columns of traces show responses to three different flash durations as indicated. Note the all-or-none characteristics of the responses. (B) Percentage of sites responding to flashes of varying durations. Data were obtained from traces similar to those in (A). Points indicate the percentage of trials ($n > 20$) with each flash duration in which responses were observed. All responses were from a single albino oocyte, at randomly chosen locations, constrained to fall within a 200 × 200-μm area of the animal hemisphere. [Reproduced by I. Parker, I. Choi, and Y. Yao, *Cell Calcium* **20**, 105 (1996), with permission of *Cell Calcium*.]

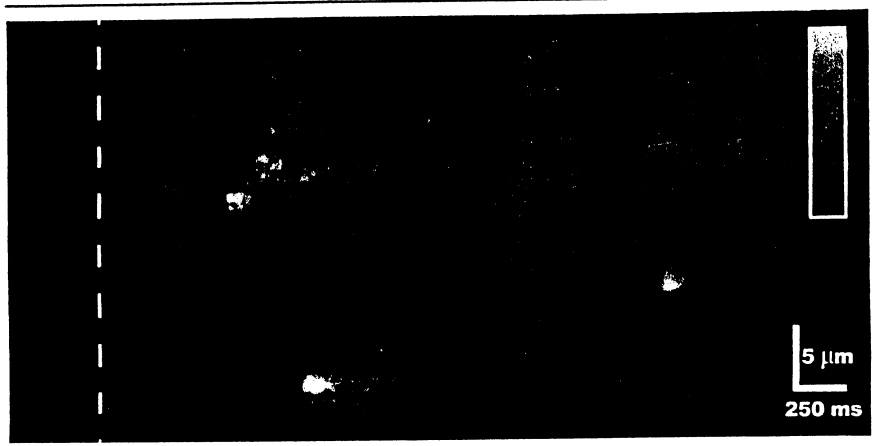

FIG. 11. Uniform photorelease of InsP_3 over a wide area evokes transient, localized, "elementary" calcium release events. The image was obtained by confocal line-scan microscopy, in which the laser spot was repeatedly scanned along a fixed line 50 μm long. Traces from successive lines are stacked from left to right so that the vertical dimension of the image represents distance along the scan line and the horizontal dimension of the image represents distance along the scan line and the horizontal dimension represents time. Increasing Ca^{2+} levels are depicted on a gray scale and are shown as a ratio relative to the resting fluorescence at each pixel before stimulation. A photolysis flash covering a spot approximately 100 μm in diameter around the scan line was applied when indicated by dashed line.

characteristic,[34] so that identical flashes delivered at different, random, locations on the oocyte evoke either no response or responses of similar amplitudes (Fig. 10A). The proportion of sites responding grows progressively as the flash duration is increased. However, this gradation occurs over a very narrow range of flash intensities, suggesting that the microscopic sensitivity to InsP_3 varies only slightly from site to site.

A different approach to obtain spatial information is to image calcium release evoked by homogeneous photolysis of c-InsP_3 over a relatively wide (50–100 μm) area, as illustrated in Fig. 11. In this case, fluorescence calcium images are obtained using a rapid (8.0 msec per line), high-resolution (0.2 μm/pixel) confocal line-scan system. Such studies reveal that homogeneous stimulation gives rise to localized "elementary" release events, originating in a stochastic manner at particular sites that probably represent clusters of InsP_3R.[13]

Finally, line-scan calcium imaging can be combined with localized photorelease induced by a focused spot from a UV laser to visualize calcium

[34] I. Parker and I. Ivorra, *Science* **250**, 977 (1990).

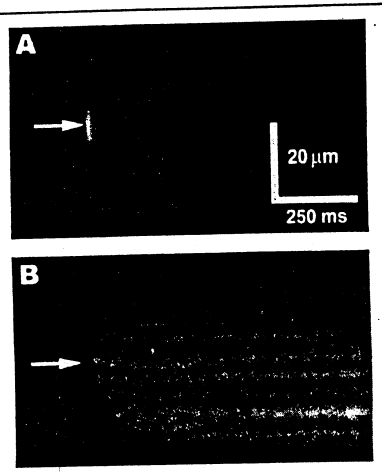

FIG. 12. Examples of UV laser "point" photolysis of caged compounds monitored by confocal line-scan imaging. (A) Control experiment monitoring fluorecsence of fluorecein photoreleased in a droplet of caged precursor. The UV laser flash was delivered at the location and time indicated by the tip of the arrowhead. (B) Ca^{2+} release evoked following photolysis of caged InsP_3 by a focused spot from a UV laser. The oocyte was loaded with Oregon green-1 (50 μM) and caged InsP_3 (5 μM), and recordings were made at a depth of 7 μm from the surface. The laser spot was positioned in the center of the line scan, and the tip of the arrowhead denotes the location and time of the flash. Line-scan imaging was performed as in Fig. 11. [Reproduced from I. Parker, N. Callamaras, and W. Wier, *Cell Calcium* **21,** 441 (1997), with permission of *Celi Calcium.*]

liberation as InsP_3 diffuses from a virtual point source. Figure 12A shows a control experiment in which fluorescein is photoreleased from a droplet of caged precursor (Molecular Probes). The image shows that fluorescein is formed almost immediately following the flash and subsequently spreads rapidly, consistent with diffusion in free solution. However, calcium liberation evoked by "point" photorelease of InsP_3 in the oocyte shows more complex characteristics (Fig. 12B). Calcium signals do not begin until after a latency of several tons of milliseconds and are first seen at the site of photorelease. Liberation then occurs at increasing distances from the photolysis spot, giving an indication of the "range of action" of InsP_3, reflecting both its diffusion and the requirement for [InsP_3] to exceed a specific threshold to evoke calcium release.

Final Comments

In summary, c-InsP_3 is an invaluable tool for the study of intracellular Ca^{2+} signaling due to the degree of control that can be exercised over the intensity, duration, and spatial extent of stimulation. This technique has been used to extend whole cell studies of the InsP_3-mediated Ca^{2+} signaling system in *Xenopus* oocytes. Combination of flash photolysis together with fluorescence Ca^{2+} imaging or membrane current recording provides a means to study the transient kinetics and modulation of spatially complex, dynamic Ca^{2+} signaling events in an intact cell. Moreover, given the flexibility, simplicity, and relative affordability of the basic apparatus necessary to conduct these experiments, the approach should be well within the reach of many investigators.

Acknowledgments

We thank Dr. Jennifer Kahle for editorial help. Financial support was provided by NIH Grant GM48071. Reprint requests and requests for further information should be addressed to Dr. Ian Parker, Laboratory of Cellular and Molecular Neurobiology, Department of Psychobiology, University of California Irvine, CA 92697-4550; e-mail, iparker@uci.edu.

[22] Characterization and Application of Photogeneration of Calcium Mobilizers cADP-Ribose and Nicotinic Acid Adenine Dinucleotide Phosphate from Caged Analogs

By KYLE R. GEE and HON CHEUNG LEE

Introduction

Two independent mechanisms for the mobilization of internal calcium stores have been identified in sea urchin eggs. The calcium-mobilizing metabolites in these mechanisms are the novel nucleotides cyclic ADP-ribose (cADPR, **1**)[1] and nicotinic acid adenine dinucleotide phosphate (NAADP, **2**),[2] derived from NAD and NADP, respectively. Cyclic ADP-ribose can function as a modulator of the calcium-induced calcium response mechanism and it also functions as a calcium messenger itself.[3] In addition to the calcium-releasing activity of cADPR in sea urchin eggs, a variety of mammalian, amphibian, and plant cells have been shown to be responsive to the molecule.[4] The calcium release mechanism activated by NAADP is

[1] H. C. Lee, T. F. Walseth, G. T. Bratt, R. N. Hayes, and D. L. Clapper, *J. Biol. Chem.* **264,** 1608 (1989).
[2] H. C. Lee and R. Aarhus, *J. Biol. Chem.* **270,** 2152 (1995).
[3] H. C. Lee, *Recent Prog. Horm. Res.* **52,** 357 (1996).
[4] H. C. Lee, *in* "CRC Series on Pharmacology and Toxicology" (V. Sorrentino, ed.), p. 31, CRC Press, Boca Raton, FL, 1995.

0076-6879/98 $25.00